Journal of Cell Science 107, 2081-2094 (1994)
Printed in Great Britain © The Company of Biologists Limited 1994

Identification of coelomocyte unconventional myosin and its association with in vivo particle/vesicle motility

Lisanne D'Andrea*, Martha A. Danon, George P. Sgourdas and Edward M. Bonder†

Department of Biological Sciences, Rutgers, The State University, University Heights, Newark, NJ 07102, USA

*Present address: Brigham and Women's Hospital, Department of Pathology, Thorn Building, Room 1423, Boston, MA 02146, USA
†Author for correspondence

SUMMARY

Sea urchin coelomocytes undergo an inducible structural transformation from petalloid to filopodial form during the 'clotting' response in sea urchins. Using a petalloid coelomocyte model, stimulated coelomocytes exhibited bidirectional particle/vesicle motility with a broad distribution of velocities, ranging from 0.02 to 0.12 $\mu m\ s^{-1}$ in the outward bound direction. Coelomocytes treated with the microtubule-disrupting drug, nocodazole, continued to exhibit outward particle/vesicle movements along linear paths with an average velocity of 0.028±0.006 $\mu m\ s^{-1}$. We partially purified a 110 kDa polypeptide possessing K^+EDTA-, Ca^{2+}-, Mg^{2+}- and F-actin-activated Mg^{2+}-ATPase activities characteristic of myosin-like motor proteins. The 110 kDa protein immuno-crossreacted with both affinity-purified, anti-brush border unconventional myosin-I polyclonal antibodies and anti-*Acanthamoeba* myosin head monoclonal antibodies. By indirect immunofluorescence, the 110 kDa unconventional myosin was localized to clusters of particles/vesicles within the perinuclear region of unstimulated coelomocytes, an area containing numerous mitochondria, acidic, lysosomal and Golgi organelles. Indirect immunofluorescence of partially transformed and filopodial coelomocytes detected a diminution of perinuclear staining with a concomitant appearance of stained linear arrays of particles/vesicles, enhanced staining of peripheral lamellae, and staining of the entire length of the filopodia. Subfractionation of unstimulated coelomocyte homogenates on linear sucrose gradients identified distinct peaks of ATPase activity associated with fractions containing conventional and 110 kDa unconventional myosin. Unconventional myosin-containing fractions were found to have numerous particles that stained with anti-brush border unconventional myosin-I antibodies and the lipophilic dye, $DiOC_6$. Thus, coelomocytes demonstrate activatable movements of particles/vesicles in cells devoid of microtubules and possess an unconventional myosin, which may be the motor protein driving particle/vesicle translocation.

Key words: motor proteins, actin cytoskeleton, organelle motility

INTRODUCTION

Myosins are mechanoenzymes endowed with the potential to perform mechanical work by utilization of the energy derived from ATP hydrolysis (Warrick and Spudich, 1987). Over the past several years, this group of proteins has grown from an original family consisting of myosin-I and -II to the present minimum of six to eight family classes with evidence of further expansion (Cheney et al., 1993; Bement and Mooseker, 1993). For convenience, the myosin 'motor' protein families are often referred to as being either conventional (myosin-II like) or unconventional (all other types) myosins (Cheney and Mooseker, 1992). Conventional myosins possess two enzymatic heads, form bipolar filaments, and demonstrate characteristic actin-activated ATPase activity (Warrick and Spudich, 1987). Unconventional myosins are structurally distinct from conventional myosins but possess similar enzymatic properties in vitro due to the conserved presence of the myosin head domain (Korn and Hammer, 1990; Pollard et al., 1991; Cheney and Mooseker, 1992; Cheney et al., 1993). To date, unconventional myosins have been identified in diverse cell types and species ranging from yeast to man (for most recent cataloging, see Cheney et al., 1993; Bement and Mooseker, 1993). Further, mounting evidence suggests that cells contain multiple myosins and studies on unconventional myosin mutants point towards potential functional redundancy (Jung and Hammer, 1990; Wessels et al., 1991; Titus et al., 1993; reviewed by Endow and Titus, 1992; Titus, 1993; Bement and Mooseker, 1993). This scenario is similar to observations with actin binding protein mutations in *Dictyostelium* that exhibited no readily apparent phenotypic defect, indicating that cells may hypothetically have a cellular fail-safe mechanism preserving essential cytoskeletal function (Witke et al., 1992; Noegel and Schleicher, 1991; Bray and Vasiliev, 1989).

The first unconventional myosin identified was the low molecular mass myosin-I isolated from *Acanthamoeba* (Pollard and Korn, 1973). Unconventional myosin-I has a single myosin-like globular head and a unique, short non-coiled coil tail domain that incorporates both light chain-

binding and lipid-binding domains (Korn and Hammer, 1990). Based on in vitro lipid binding, reconstituted vesicle motility, and immunolocalization studies, unconventional myosin-Is have been implicated in actin-membrane motility events such as phagocytosis, pseudopodial extension and vesicle motility (see Pollard et al., 1991; Cheney and Mooseker, 1992; Titus, 1993, for recent reviews). Observations in *Acanthamoeba* (Baines et al., 1992; Yonemura and Pollard, 1992), *Drosophila* embryos (Kellerman and Miller, 1992), mammalian tissue culture cells (Wagner et al., 1992) and intestinal epithelial cells (Fath and Burgess, 1993) provide the strongest evidence that unconventional myosins are at least intracellularly positioned to participate in the cytoplasmic transport of vesicle cargo. Interestingly, *Acanthamoeba* unconventional myosin-1C has been demonstrated to play a role in contractile vacuole function either through a direct contractile mechanism (Doberstein et al., 1993) or possibly through regulation of water transporters (Bement and Mooseker, 1993). Thus, in addition to a role in traditional motility, the unconventional myosins may serve in other, unidentified, cellular capacities.

To investigate myosin's potential for mediating intracellular cargo transport, we turned to petalloid coelomocytes, which are primitive non-specific immune cells circulating in the coelomic cavity of sea urchins that function in phagocytosis of bacteria and formation of clots (Coffaro and Hinegardner, 1977; Yui and Bayne, 1983). At the site of bodily injury, petalloid coelomocytes possessing numerous bladder-like lamellae are transformed into cells having abundant slender filopodial projections across their entire surface. Coelomocytes also undergo particle/vesicle degranulation leading to the release of agglutinins that facilitate cell adhesiveness, leading to the formation of a fibrous plug sealing the wound (Endean, 1966; Johnson, 1969; Canicatti et al., 1992; Ryoyama, 1974). Petalloid-to-filopodial transformation may consist of two distinct steps, one involving perinuclear particle/vesicle translocation and exocytosis (Endean, 1966; Johnson, 1969), and the other the well characterized transformation of the actin cytoskeleton from lamellar bundles and meshworks to long slender actin filament bundles supporting filopodia (Edds, 1980). This mechanism of cellular transformation is analogous to the activation of platelets during clot formation in the circulatory system of higher animals (Allen et al., 1979).

In this study, the coelomocyte model was used to investigate the cellular mechanisms of intracellular particle/vesicle motility. Coelomocyte preparations spread on coverslips are capable of stimulus-induced intracellular particle/vesicle motility in the absence of filopodial formation. Several discrete velocities for particle/vesicle translocation from a perinuclear position outwards into the spread lamellae were identified. Disruption of microtubules did not abolish particle/vesicle motility but instead altered the particle/vesicle velocity profile. Thus, experimentally, the coelomocyte model permitted identification of an actin microfilament-dependent motility pathway that, in turn, suggested a role for 'myosin motor' proteins. A 110 kDa polypeptide has been partially purified and characterized as being immunologically and enzymatically related to the unconventional myosin protein family. By indirect immunofluorescence, coelomocyte unconventional myosin was localized to particles/vesicles within the perinuclear region of untransformed coelomocytes. Interestingly, during the transformation process, unconventional myosin-associated particles/vesicles were no longer restricted to the perinuclear endoplasm but were observed within lamellae and, in fully transformed cells, unconventional myosin was observed along the length of newly formed filopodia. The inducible membrane-cytoskeletal dynamics observed in coelomocytes may provide a model system with which to examine the functional role of myosin isoforms during the rapid restructuring of the actin-membrane cytoarchitecture following stimulus-induced transformation.

MATERIALS AND METHODS

Materials

Strongylocentrotus purpuratus were purchased from either Bodega Bay Marine Labs (Bodega Bay, CA) or Marinus Inc. (Long Beach, CA) and maintained in laboratory saltwater aquaria. Primary antibodies were kind gifts from Drs K. Collins and P. Matsudaira (affinity-purified, anti-chicken brush border unconventional myosin-I polyclonal antibody; Collins et al., 1990), Dr T. Pollard (anti-*Acanthamoeba* myosin-II monoclonal antibody-M2.18; Kiehart et al., 1984; Carboni et al., 1988), Dr T. Keller (anti-chicken brush border myosin-II polyclonal antibody), and Dr J. Sellers (anti-platelet conventional myosin-II antibodies). Fluorescein- and rhodamine-conjugated secondary antibodies were obtained from Sigma Chemicals (St Louis, MO). Rhodamine-phalloidin was purchased from Molecular Probes (Eugene, OR). Alkaline phosphatase-conjugated secondary antibodies were from Hyclone Laboratories (Logan, Utah) or Cappel Research Products (Durham, NC). All other chemicals of reagent grade or better were purchased from either Baker or Sigma.

Particle/vesicle motility and video light microscopy

S. purpuratus coelomocytes were allowed to settle onto glass coverslips of perfusion chambers for 10-30 minutes and then challenged with hypotonic buffer (0.3 M NaCl, 5 mM $MgCl_2$, 20 mM HEPES, pH 7.4) to induce particle/vesicle motility. Radial microtubule networks were disrupted by exposing coelomocyte preparations to hypotonic buffer containing 20 μM nocodazole (Sigma Chemicals, St Louis, MO) for 40-60 minutes and then rates of particle/vesicle motility were analyzed. Companion preparations were subjected to immunofluorescence for localization of tubulin and actin. Alternatively, coelomocytes were exposed to nocodazole in isotonic buffer (0.5 M NaCl, 5 mM $MgCl_2$, 20 mM HEPES, pH 7.4) and then particle/vesicle motility was induced by hypotonic shock after 45 minutes. Coelomocytes were observed on a Zeiss Axiophot fitted with DIC optics using a Plan-Neo ×100 (NA 1.3) objective lens. Images were collected using a Hamamatsu Newvicon camera and recorded with either a time-lapse or a standard S-VHS video recorder. For some observations, video images were frame averaged (8 frames) and digitally enhanced using a Quantex image processor prior to recording. Rates of movement were obtained from real-time video recordings of individual coelomocytes by measuring single continuous movements of a given particle. Only those particles moving radially outwards from the perinuclear region were measured, and 1-3 movements were used per particle. Data were analyzed with Sigma Plot Software (Jandel Scientific, Corte Madera, CA), using the Marquardt-Levenberg non-linear curve-fitting algorithm. Video images were photographed directly off a monitor using Kodak TRI-X PAN 35 mm film or printed using a Hitachi VY170A videoprinter.

Protein and particle/vesicle isolation

Unconventional myosin

S. purpuratus coelomocytes from non-ripe males and non-gravid females were isolated by a modification of the method of Hyatt et al. (1984). All steps were carried out at 4°C. Coelomic fluid was collected

in a 1:1 volume ratio with an anticoagulation buffer containing 0.5 M NaCl, 50 mM EGTA, 26 mM KCl and 0.1 M Tris-HCl, pH 8.0. The suspension was filtered through cheesecloth, layered over anticoagulant buffer containing 0.8 M sucrose and centrifuged for 5 minutes at 3000 ***g***. Coelomocytes present at the sucrose interface and in the supernatant were collected, diluted 1:1 with anticoagulant buffer and centrifuged for 30 minutes at 9,000 ***g***. Pellets of coelomocytes were resuspended in either anticoagulant buffer or isotonic buffer (0.5 M NaCl, 5 mM $MgCl_2$, 20 mM HEPES, pH 7.4) and washed twice by repeated centrifugation. Approximately 2.5 ml pellets of coelomocytes were homogenized at 4°C in a 20-fold volume excess of ice-cold homogenization buffer (20 mM HEPES, pH 7.4, 2 mM $MgCl_2$, 1 mM EGTA, 75 mM KCl, 250 mM sucrose, 2 mM ATP, 1 mM DTT, 10 mM TAME, 10 mM benzamidine, 8 μg/ml aprotinin, 0.4 μg/ml SBTI, 10 μg/ml leupeptin, 80 μg/ml TPCK, 5 μg/ml pepstatin A) using a glass Dounce homogenizer (Kontes Glassware, Vineland, NJ). The homogenate was centrifuged at 9000 ***g*** for 30 minutes and the supernatant was further centrifuged at 100,000 ***g*** for 1.5 hours. The 100,000 ***g*** supernatant, containing unconventional myosin, was concentrated 10-fold using Aquacide and dialyzed into buffer Q (10 mM imidazole, pH 7.3, 0.1 mM $MgCl_2$, 1 mM EGTA, 100 mM NaCl) containing 2.5 mM TAME, 2.5 mM benzamidine, 1 mM ATP, 1 mM DTT, 8 μg/ml aprotinin, 5 μg/ml leupeptin, 5 μg/ml pepstatin A, 40 μg/ml PMSF. The extract was loaded onto a 32 cm × 1.75 cm S-200 column (Pharmacia Fine Chemicals, Piscataway, NJ) previously equilibrated in buffer Q. Fractions containing coelomocyte unconventional myosin (as determined by SDS-PAGE, immunoblot analysis, and ATPase assays) were pooled, dialyzed into fresh buffer Q and loaded onto a 1 cm × 1.75 cm Q-Sepharose column (Pharmacia Fine Chemicals, Piscataway, NJ). The column was eluted stepwise with 100, 250 and 600 mM NaCl in buffer Q. Highly enriched fractions of unconventional myosin eluting at 600 mM NaCl were pooled and stored on ice for further use.

Particle isolation

Petalloid coelomocytes were obtained by the procedure outlined above. Approximately 200 μl of packed coelomocytes were homogenized at 4°C in 1 ml of 5% sucrose in buffer H (20 mM HEPES, pH 7.4, 2 mM $MgCl_2$, 75 mM KCl, 1 mM EGTA, 2 mM ATP, 1 mM DTT, 8 μg/ml aprotinin, 1 mM benzamidine and 1 mM TAME) using a glass Dounce homogenizer. The extract was microfuged for 2-5 minutes to remove large particulates. The resulting supernatant was layered onto a 15 ml linear 5% to 25% sucrose gradient in buffer H, topped with 1 ml of 2.5% sucrose in buffer H and centrifuged for 14 hours at 25,000 rpm in a Beckman SW 28 rotor. Samples (500 μl) were sequentially extracted from the top to the bottom of the gradient. Fractions were assayed for total protein by the method of Bradford (1976), analyzed by SDS-PAGE, and immunoblotted.

Fluorescence microscopy

Immunofluorescence localization of unconventional myosin

Spread petalloid *S. purpuratus* coelomocytes were obtained by allowing the cells to attach to glass coverslips and nonadherant cells were removed by washing with isotonic buffer (0.5 M NaCl, 5 mM $MgCl_2$, 20 mM HEPES, pH 7.4). Partially and fully transformed coelomocytes were obtained by hypotonically challenging and fixing the cells in suspension prior to adhering cells to coverslips. Coelomocytes were fixed at room temperature for 45 minutes using 0.1% glutaraldehyde and 3% paraformaldehyde in either isotonic or hypotonic buffer. Free aldehyde was quenched by a 45 minute incubation at room temperature in the appropriate buffer containing 150 mM glycine. The fixed cells were then incubated for 60 minutes in blocking buffer containing 1% BSA, 0.1% Triton X-100, and 5% fetal calf serum, rinsed with PBS, and incubated for 1 hour at room temperature with affinity-purified, anti-brush border unconventional myosin-I polyclonal antibodies (1:10 dilution). The primary antibody was then removed, coverslips were washed extensively in PBS and probed for 1 hour with fluorescein- or rhodamine-conjugated secondary antibodies at a dilution of 1:50. Coverslips were rinsed extensively in PBS and mounted on glass slides in glycerol/phenylenediamine (Platt and Michael, 1983). Control preparations were fixed, quenched, blocked, washed and incubated with either non-immune serum or secondary antibody only. Fluorescent preparations were examined using a Zeiss Axiophot microscope equipped with epi-fluorescence illumination, and photomicrographs were recorded on either Kodak Tri-X Pan film processed in Acufine developer or Kodak T-Max film processed in T-Max developer.

F-actin staining

Coelomocytes were settled on coverslips, fixed, probed with 50 nM rhodamine-phalloidin for 1 hour in the dark and processed as described above.

Anti-tubulin staining

Coelomocytes were placed on coverslips and fixed for microtubules in 3% formaldehyde as described by Edds (1984). Coverslips were incubated for 1 hour at room temperature with an anti-tubulin monoclonal antibody (Sigma Chemicals, St Louis, MO) at a 1:250 dilution followed by a 1 hour incubation in FITC-goat anti-mouse secondary antibody diluted 1:50. Control preparations included incubation of coverslips in secondary antibody only.

Immunofluorescence of isolated particles

Samples from sucrose gradients identified as containing unconventional myosin on immunoblots were fixed in suspension for 30 minutes at room temperature with 3% formaldehyde in buffer H and allowed to settle onto polylysine-coated coverslips. Coverslips were washed with PBS and blocked for 30 minutes in 1% fetal calf serum and 3% BSA in PBS. Coverslips were then incubated in a 1:10 dilution of affinity-purified, anti-brush border unconventional myosin-I antibody or a 1:50 dilution of anti-myosin-II antibody for 1 hour at room temperature. Coverslips were washed extensively with PBS and incubated for 1 hour at room temperature in a 1:50 dilution of rhodamine- or fluorescein-conjugated goat anti-rabbit secondary antibody. Control preparations included incubating coverslips in the presence of secondary antibody only. Coverslips containing unfixed preparations from sucrose gradient fractions were also stained with 2 μM $DiOC_6$ (Molecular Probes, Eugene, OR) in isotonic buffer for 30 minutes in the dark. Coverslips were then washed extensively and mounted as described above.

Gel electrophoresis and immunoblot analysis

SDS-PAGE was performed according to the method of Laemmli (1970) using mini-slab gels (Matsudaira and Burgess, 1978). SDS-gels were scanned using an LKB XL laser densitometer. Proteins electrophoresed on 7.5% to 15% gradient gels were transferred to nitrocellulose (Towbin et al., 1979) and blocked for 5 hours at room temperature in TTBS (20 mM Tris-HCl, pH 7.5, 150 mM NaCl, 0.2% Tween-20, 0.02% NaN_3) containing 1% fetal calf serum and 3% BSA. Nitrocellulose blots were then washed 5-10 times in TTBS and 5-10 times in TBS (20 mM Tris-HCl, pH 7.5, 150 mM NaCl, 0.02% NaN_3). The blots were probed with primary antibody overnight in the cold, washed 5 times in TTBS, 5 times in TBS followed by a 4 hour incubation in a 1:1000 dilution of alkaline phosphatase-conjugated goat anti-mouse or goat anti-rabbit secondary antibody. The blots were developed in a solution containing 60 μg/ml nitro blue tetrazolium and 60 μg/ml bromochloro-indoyl phosphate (Dubreuil et al., 1987).

ATPase assays

ATPase activity through 60 minutes at 35°C was determined according to the method of Pollard and Korn (1973). Assay conditions were: 20 mM imidazole, pH 7, 0.2 mM DTT, 0.575 M KCl, 2 mM EDTA, for K^+EDTA; 20 mM imidazole, pH 7, 0.2 mM DTT, 0.575 M KCl, 0.1 mM $MgCl_2$, 1 mM $CaCl_2$, for Ca^{2+}; 20 mM imidazole,

pH 7, 0.2 mM DTT, 0.575 M KCl; or 0.05 M KCl, 5 mM EGTA, 5 mM $MgCl_2$, for Mg^{2+}. In experiments examining the F-actin-activated Mg^{2+}-ATPase activity, the final concentration of F-actin was 40 μM. ATPase activity due to F-actin was measured in control preparations lacking myosin and subsequently subtracted from the activity of the myosin-containing experimental group.

RESULTS

In vivo motility of particles/vesicles in the absence of microtubule tracks

Hypotonic shock of coelomocytes 'in suspension' results in fully transformed cells possessing numerous elongate filopodia, giving transformed cells the appearance of adult spiny sea urchins. However, once petalloid coelomocytes tightly attach and spread on a coverglass they are no longer able to fully form surface filopodia in response to hypotonic shock. Instead, adherent cells demonstrate perinuclear particle/vesicle motility and lamellar motility including membrane extension/retraction, ruffling, microspike formation/retraction, retrograde cortical flow and inductopodia formation (Fig. 1; Edds, 1993; Forscher et al., 1992). Upon challenge with hypotonic buffer, particle/vesicle motility was enhanced within the perinuclear region and numerous particles/vesicles began to move radially outwards along linear tracks into the lamellae (Fig. 1). Phase-contrast microscopy of activated coelomocytes identified the outwardly moving particles/vesicles as being primarily phase-dense (data not shown; also see Figs 4, 7). Recently, Henson et al. (1992) demonstrated that many of the perinuclear and lamellar particles represent acidic compartments, endosomes, Golgi and mitochondria. Particles/vesicles migrating outwards into the lamella occasionally paused, exhibited saltatory movements, and then resumed movement. In some cases, it is possible to detect radially aligned linear elements that appear to function as the 'tracks' for translocation of cargo (Fig. 1A, see bracket).

Anti-tubulin antibody staining of spread coelomocytes identified a dense basket of microtubules within the perinuclear region and a radial array of microtubules extending outward into the lamellae (Fig. 1E). Rhodamine-phalloidin staining detected an extensive meshwork of actin filaments forming a scaffold for the lamellae, along with actin filament bundles extending outwards from the center of the cell (Fig. 1F).

Measurements of the rates of particle/vesicle movements in control coelomocytes revealed a very broad distribution of outward velocities ranging from 0.02 to 0.12 μm s^{-1} (Fig. 3A, below) with an average velocity of 0.053 μm s^{-1} ± 0.031 (mean ± s.d.; *n*=100) for the entire population. Inspection of the data suggested that the measured rates of movement might not readily be described by a single Gausian distribution. Data analysis using a non-linear curve-fitting algorithm verified that the velocity profile was best correlated with three individual Gausian distributions, indicating the possible presence of three discrete populations of moving particles/vesicles having potentially different motor protein associations.

To distinguish between particles/vesicles translocating along microtubule or actin microfilament tracks, coelomocytes were treated with 20 μM nocodazole to disassemble radial microtubules (Edds, 1977). Nocodazole-treated coelomocytes generally appeared morphologically indistinct from control cells and were able to undergo membrane ruffling and formation of microspikes (Fig. 2). However, nocodazole-treated cells demonstrated enhanced membrane activity with extensive cortical flow and inductopodial activity (Fig. 2A,D). Companion preparations probed with anti-tubulin antibodies verified the absence of radial microtubules, with only a small residual microtubule basket in the perinuclear region (Fig. 2E). Nocodazole-treated cells exhibited apparently unaltered actin filament meshworks and bundles in lamellae (Fig. 2F). In the absence of radial microtubules, particles/vesicles continued to translocate radially outwards; however, the extent of translocation and degree of motility were visibly reduced when compared with control preparations. The measured velocities were tightly grouped, with an average velocity of 0.028±0.006 μm s^{-1} (mean ±s.d.; *n*=97; Fig. 3B), and were well correlated with a single Gausian distribution that coincided with the major slow velocity peak measured in non-nocodazole-treated control coelomocytes.

Identification of coelomocyte myosins

Particle/vesicle motility in the absence of microtubule networks indicated the existence of a myosin-driven cargo transport system. Early observations by Edds (1977) demonstrated the presence of a high molecular mass polypeptide in coelomocyte extracts that co-migrated with skeletal muscle myosin on SDS-gels. In preliminary studies, we identified coelomocyte conventional myosin-II (D'Andrea, 1993) and used an anti-conventional brush border myosin-II antibody to examine the cellular localization of this myosin isoform (Fig. 4). Conventional myosin-II was diffusely localized throughout the cytoplasm and there appeared to be some suggestion that myosin-II was associated with lamellar networks (Fig. 4B) that might correspond with the distribution of actin networks and bundles (see Figs 1, 2). There was no clear detectable association of myosin-II with phase-dense perinuclear particles (Fig. 4). Therefore, since myosin-II appeared not to be associated with migrating particles/vesicles, coelomocytes were fractionated and examined for actin-activated ATPase activities that corresponded to the presence of polypeptides recognized by anti-unconventional myosin antibodies. Subfractionation of coelomocyte extracts using S-200 and Q-Sepharose column chromatography yielded a partially purified, enriched preparation of a 110 kDa polypeptide (Fig. 5A). Based on protein determinations and scanning densitometry of SDS-PAGE, the purification protocol yielded ~125 μg of the 110 kDa polypeptide when starting with 2-3 ml of coelomocytes. The 110 kDa-enriched fractions exhibited an active K^+EDTA ATPase that was suppressed by Ca^{2+} or Mg^{2+} (Table 1). At high salt con-

Table 1. ATPase activity of coelomocyte 110 kDa unconventional myosin

	ATPase activity*			
			Mg^{2+}	
KCl concn	K^+ EDTA	Ca^{2+}	–Actin	+Actin
0.575 M	224	68	83	100
50 mM	–	–	24	249

Enriched 110 kDa unconventional myosin from Q-Sepharose eluate was used.

*All activities measured in nmol min^{-1} mg^{-1}.

centration (0.575 M KCl) there was minimal enhancement of ATPase activity in the presence of F-actin. However, at low ionic strength (0.05 M KCl), F-actin accelerated the ATPase activity by a factor of approximately 10 (Table 1). Data presented in Table 1 are calculated for total protein (200 μg/ml) and thus may underestimate the ATPase activity of 110 kDa, since in these preparations it represents 25% of the total protein. Additional kinetic analysis of the observed ATPase is required to characterize the enzymatic properties of 110 kDa. The observed ATPase activities of the 110 kDa polypeptide-containing fractions were characteristic of myosin-like enzymes and the salt-dependent actin activation of ATPase activity was reminiscent of the behavior of brush border unconventional myosin-I (Collins et al., 1990; Conzelman and

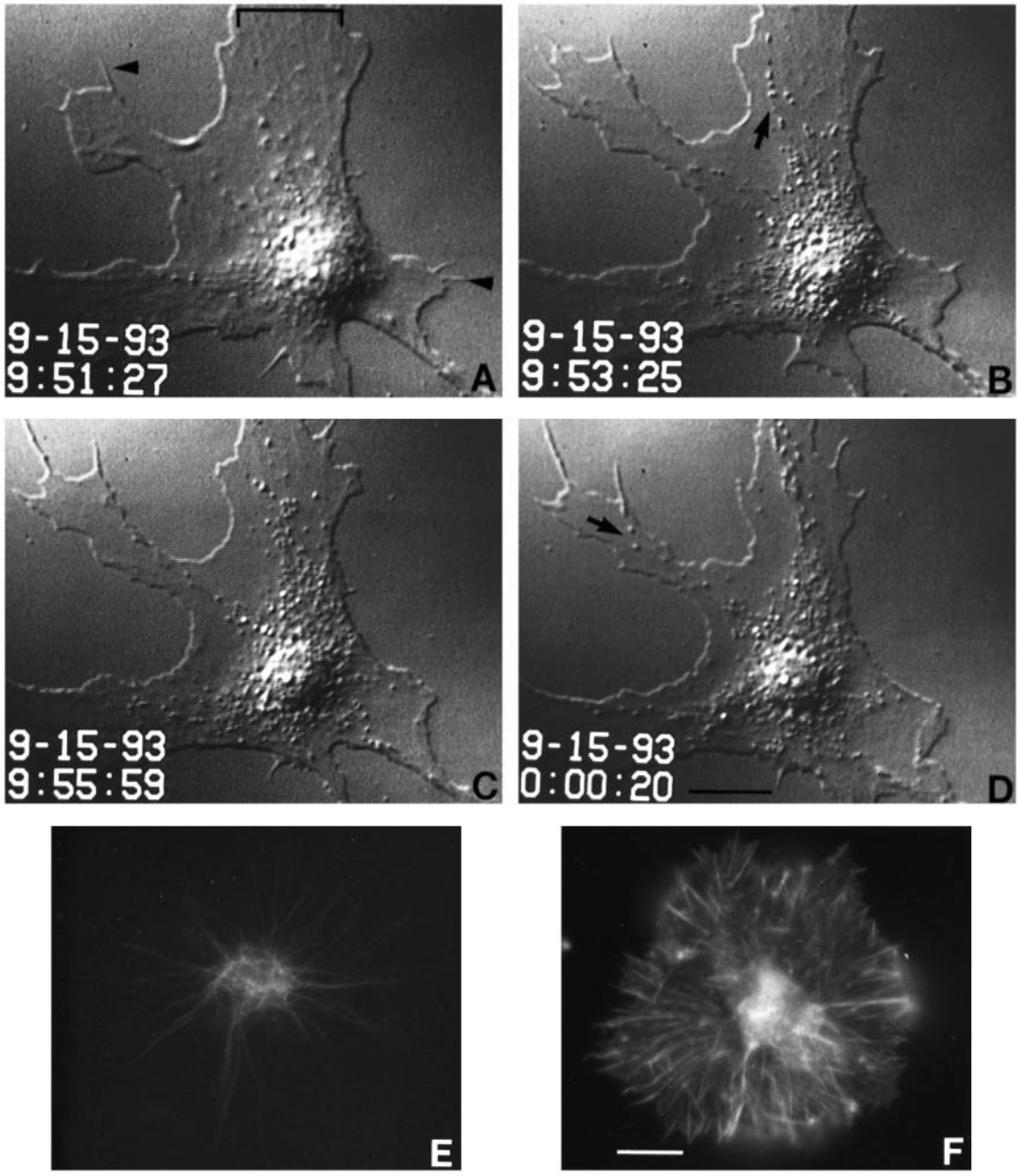

Fig. 1. (A-D) Video time-lapse sequence of *S. purpuratus* coelomocyte particle/vesicle motility following hypotonic shock. Prior to treatment with hypotonic buffer (A) the coelomocyte possessed short filopodia and microspikes (arrowheads), an array of radially aligned intracellular 'tracks' (see bracket), and numerous perinuclear particles/vesicles. Following hypotonic shock (B-D), there ensued a massive migration of particles/vesicles outwards into the spread lamellae often along common linear paths (see arrows). (E) Fluorescence micrograph showing anti-tubulin antibody staining of an equivalent preparation depicting a central basket of perinuclear microtubules with outwardly radiating microtubules. (F) Companion cell stained with rhodamine-phalloidin showing the dense network of actin filaments and actin filament bundles within flattened lamellae. Bar, 10 μm.

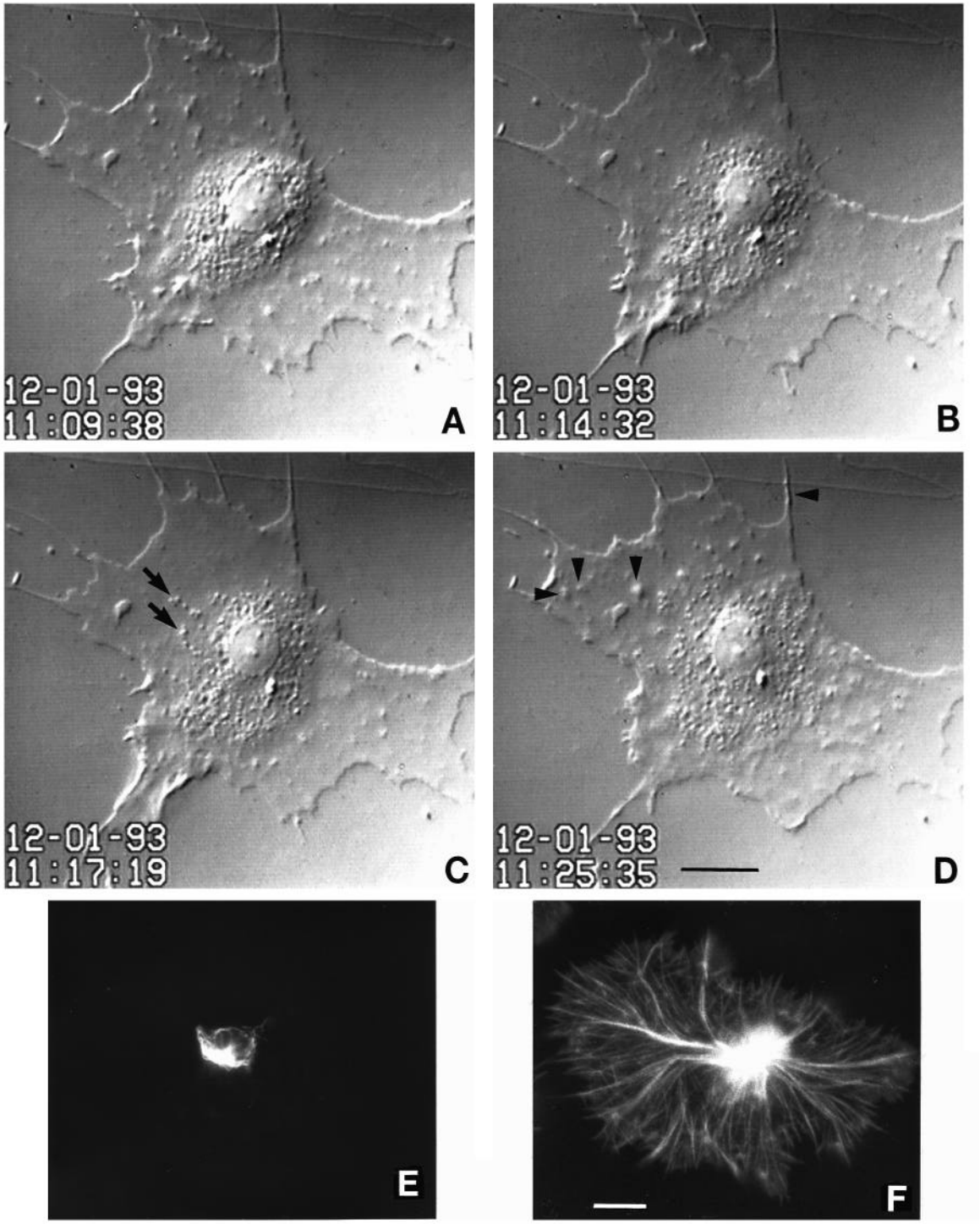

Fig. 2. (A-D) Video time-lapse and fluorescence cytochemical analysis of nocodazole-treated coelomocytes. Immediately after treatment with hypotonic buffer (A), the tightly packed perinuclear particles/vesicles become more active and begin to move outward into the lamellae (B-D) often along the same 'tracks' (C, arrows). Additionally, nocodazole-treated cells exhibited enhanced 'membrane' activity with the formation of numerous ruffles, microspikes and inductopodia (see D, arrowheads). (E) Fluorescence micrograph showing anti-tubulin staining of a companion nocodazole-treated coelomocyte. Nocodazole treatment resulted in a loss of radiating microtubules in the lamellae with only remnants of microtubule fragments surrounding the nucleus. (F) Rhodamine-phalloidin staining of a nocodazole-treated coelomocyte. Bar, 10 μm.

Mooseker, 1987; Krizek et al., 1987; Wolenski et al., 1993).

Immunoblot analysis of the 110 kDa polypeptide-containing fractions using either anti-chicken brush border conventional myosin-II or anti-platelet conventional myosin-II polyclonal antibodies did not detect the presence of conventional myosin-

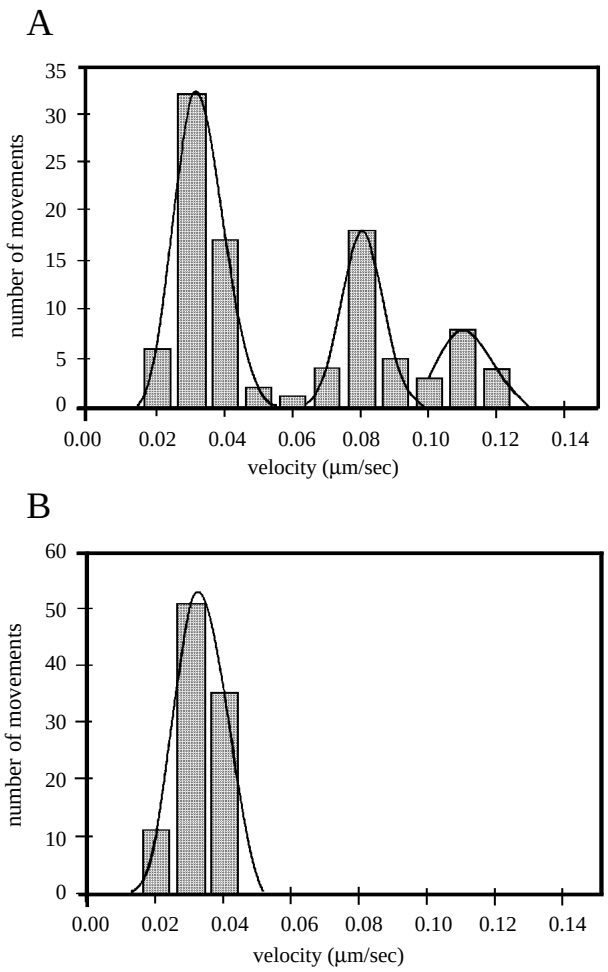

Fig. 3. Analysis of in vivo coelomocyte particle/vesicle motility. Rates of particle/vesicle movements were calculated by measuring the distance of a given movement, divided by the time elapsed between video frames. (A) Histogram of particle/vesicle velocities in control cells, overlaid (continuous line) with the correlated Gausian distributions obtained using a non-linear curve-fitting algorithm. Notice, that the data are well fit to three separate Gausian distributions. (B) Histogram of particle/vesicle movements taken from nocodazole-treated cells. Note the single Gausian velocity distribution in the absence of microtubules.

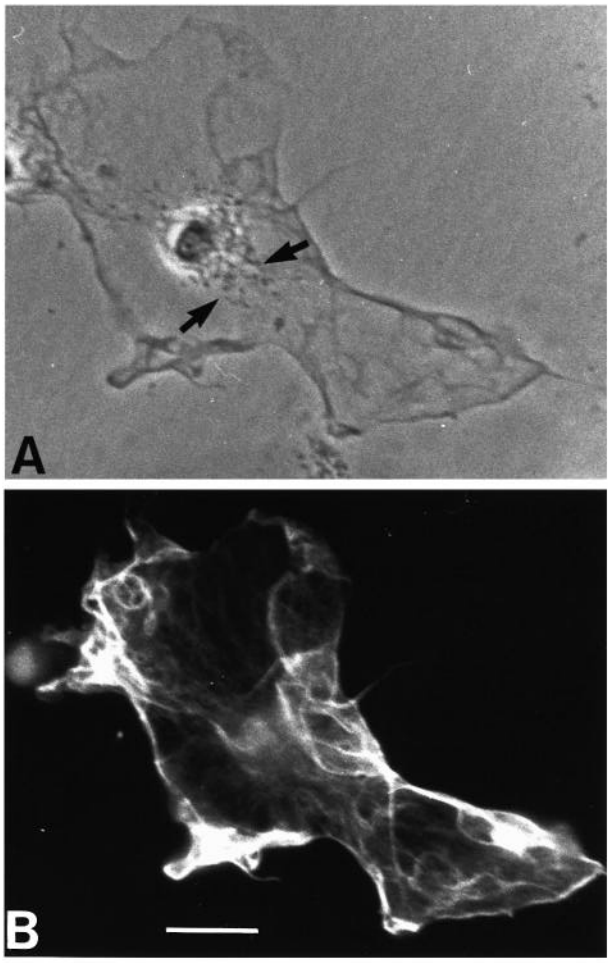

Fig. 4. Indirect immunofluorescence localization of conventional myosin-II in petalloid coelomocytes. (A) Phase-contrast micrograph of a spread coelomocyte. In this particular cell, there is a small population of phase-dense particles/vesicles that have slightly migrated into the lamellae (see arrows). (B) Fluorescence micrograph of the cell in A labeled with an anti-brush border conventional myosin-II antibody. Myosin-II exhibited a diffuse cytoplasmic staining with some indication of localization to networks or bundles within the lamellae. Noteworthy is the observation that there appears to be no discrete staining of either the phase-dense particles/vesicles that migrated into the lamella or those present in the perinuclear region. Bar, 10 μm.

II in these preparations (data not shown; D'Andrea, 1993). To test for the possibility that the 110 kDa polypeptide was related to unconventional myosin, two different antibody preparations were used to test for immunocrossreactivity. Anti-*Acanthamoeba* myosin head-specific monoclonal antibodies, previously shown to be highly specific for chicken brush border unconventional myosin-I (Carboni et al., 1988), demonstrated crossreactivity with the 110 kDa polypeptide (Fig. 5B, lane 1) but not coelomocyte myosin-II. Further, an affinity-purified, polyclonal antibody raised against brush border unconventional myosin-I also demonstrated crossreactivity with the 110 kDa polypeptide (Fig. 5B, lanes 2 and 3). Given the observation that preparations enriched for 110 kDa exhibited myosin-like ATPase activity and that the 110 kDa polypeptide demonstrated immunocrossreactivity with two different anti-unconventional myosin antibodies, we suggest that the 110 kDa polypeptide is related to the unconventional myosin family of proteins.

Distribution of unconventional myosin in coelomocytes: localization to intracellular particles/vesicles

Spread coelomocytes probed with affinity-purified anti-brush border myosin-I antibodies revealed bright fluorescence staining of the perinuclear region (Fig. 6A,A′) and a faint, broad band of fluorescence towards the outer edges of flattened lamellae (Fig. 6B). Perinuclear staining appeared to co-localize with clusters of phase-dense and phase-lucent particles/vesicles and at higher magnification it was possible to identify clearly individual brightly stained particles (Fig. 6B,C,

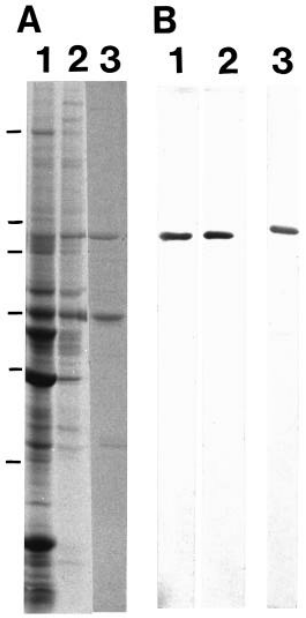

Fig. 5. Coelomocyte unconventional myosin. (A) SDS-PAGE, summary of enriched unconventional myosin preparation: S-200 column load (lane 1); Q-Sepharose column load (lane 2); enriched unconventional myosin fraction from Q-Sepharose eluate (lane 3). Densitometric analysis revealed that the 110 kDa polypeptide represented ~25% of the total protein in the extract. (B) Western blot analysis. The same fraction as in A, lane 3 was probed with an anti-*Acanthamoeba* myosin head-piece-specific monoclonal antibody (lane 1) and with an affinity-purified, anti-brush border unconventional myosin-I polyclonal antibody (lane 2). Whole coelomocyte extract was probed with the anti-brush border unconventional myosin-I polyclonal antibody (lane 3). Molecular mass markers were myosin (205 kDa), β-galactosidase (116 kDa), phosphorylase *b* (95 kDa), bovine serum albumin (66 kDa), ovalbumin (45 kDa), and carbonic anhydrase (29 kDa).

arrows). Additionally, phase-dense particles/vesicles and clusters in the peripheral lamellae were also labeled with anti-brush border unconventional myosin-I antibodies (Fig. 6A,A′, arrows). Recently, Henson et al. (1992) reported that phase-dense particles within the perinuclear region and lamellae represent populations of membraneous organelles, including Golgi, lysosomes, endoplasmic reticulum and acidic vesicles. The observed localization of unconventional myosin was in distinct contrast to the staining pattern observed for conventional myosin-II (Fig. 4).

Once coelomocytes are fully attached to glass they do not readily transform from the petalloid to the filopodial form. In order to determine the localization of the 110 kDa unconventional myosin during the transition from petalloid to filopodial form, we treated coelomocytes with hypotonic shock in suspension and then processed partially and fully transformed cells for immunofluorescence. Partially transformed cells no longer demonstrated the distinct patches of fluorescence in the perinuclear region typical of spread coelomocytes (Fig. 7A,A′). Instead, the level of fluorescence associated with lamellae was markedly increased and phase-dense particles/vesicles appeared to be linearly aligned within the transforming lamella (Fig. 7A,A′).

Examination of fully transformed, filopodial cells revealed anti-unconventional myosin staining along the entire length of the recently formed filopodia (Fig. 7B,B′). At this point very few perinuclear particles/vesicles were observed and there was a loss of the clustered perinuclear anti-unconventional myosin staining seen in petalloid cells. However, light perinuclear staining persisted but it appeared to be uniformly distributed either over or within what remained of the perinuclear zone.

Isolation of unconventional myosin-associated particles

In an effort to begin characterizing the particles/vesicles associated with coelomocyte unconventional myosin, extracts of non-stimulated coelomocytes were subfractionated on linear 5% to 25% sucrose gradients (Fig. 8A) and the resulting gradient fractions were subjected to K^+EDTA ATPase assays, immunoblotting, and light microscopy. Two peaks of ATPase activity were detected, one at ~10% sucrose and a second slightly more active at ~15% sucrose (Fig. 8A). Immunoblotting across the gradient, using a mixture of anti-conventional and unconventional myosin antibodies, identified the first peak as corresponding to the presence of unconventional 110 kDa myosin and the second peak to conventional 205 kDa myosin (Fig. 8B). The myosin-II peak sedimented at approximately the same sucrose density as observed for echinoderm egg myosin-II minifilaments (Mabuchi, 1976).

DIC microscopy of sucrose gradient fractions containing the 110 kDa unconventional myosin revealed numerous small particles similar in size to the motile particles/vesicles observed within hypotonically treated cells (Fig. 9). When examined by indirect immunofluorescence, all of the particles visible by DIC were labeled with affinity-purified, anti-brush border unconventional myosin-I antibodies (Fig. 9A,A′). Conversely, there was no detectable staining of the particles with anti-conventional myosin-II antibodies (Fig. 9B,B′). We do not know what percentage of the total 110 kDa polypeptide in the fractions is bound to the particles and future experimentation will be needed to make this determination. Additionally, the particles detected by DIC were found to stain with $DiOC_6$ (Fig. 9C), a lipophilic dye routinely used as a diagnostic for membrane compartments and organelles (Terasaki et al., 1984; Wilson, 1985), suggesting that the isolated particles were of vesicular origin.

DISCUSSION

Over the last several years, biochemical, molecular biological and molecular genetic studies have identified a wealth of 'myosin-like' mechanoenzymes that have the potential to serve as motors in the transport of cellular cargo along actin filaments (Cheney et al., 1993; Endow and Titus, 1992; Titus, 1993). Further, evidence suggests that individual cells may contain multiple motor proteins that have their own cellular role and, in addition, could functionally substitute for another myosin (Cheney et al., 1993; Endow and Titus, 1992; Titus, 1993). Apart from the clear demonstration of the vital role of conventional myosin-II in cytokinesis and the identification of *Acanthamoeba* myosin-1C regulation of contractile vacuole activity (Doberstein et al., 1993), defining the physiological roles for the unconventional myosins has been elusive (see Bement and Mooseker, 1993; Titus, 1993 for reviews). However, experimental studies demonstrating that unconventional myosins are able to bind and transport lipid membranes (Adams and Pollard, 1986; Zot et al., 1992; Doberstein and Pollard, 1992; Hayden et al., 1990) are localized to a number of different intracellular membranes (Baines et al., 1992), and are associated with a subset of Golgi vesicles (Fath and Burgess, 1993), give a strong indication that unconventional myosins could participate in transport and motility of cellular vesicle cargo.

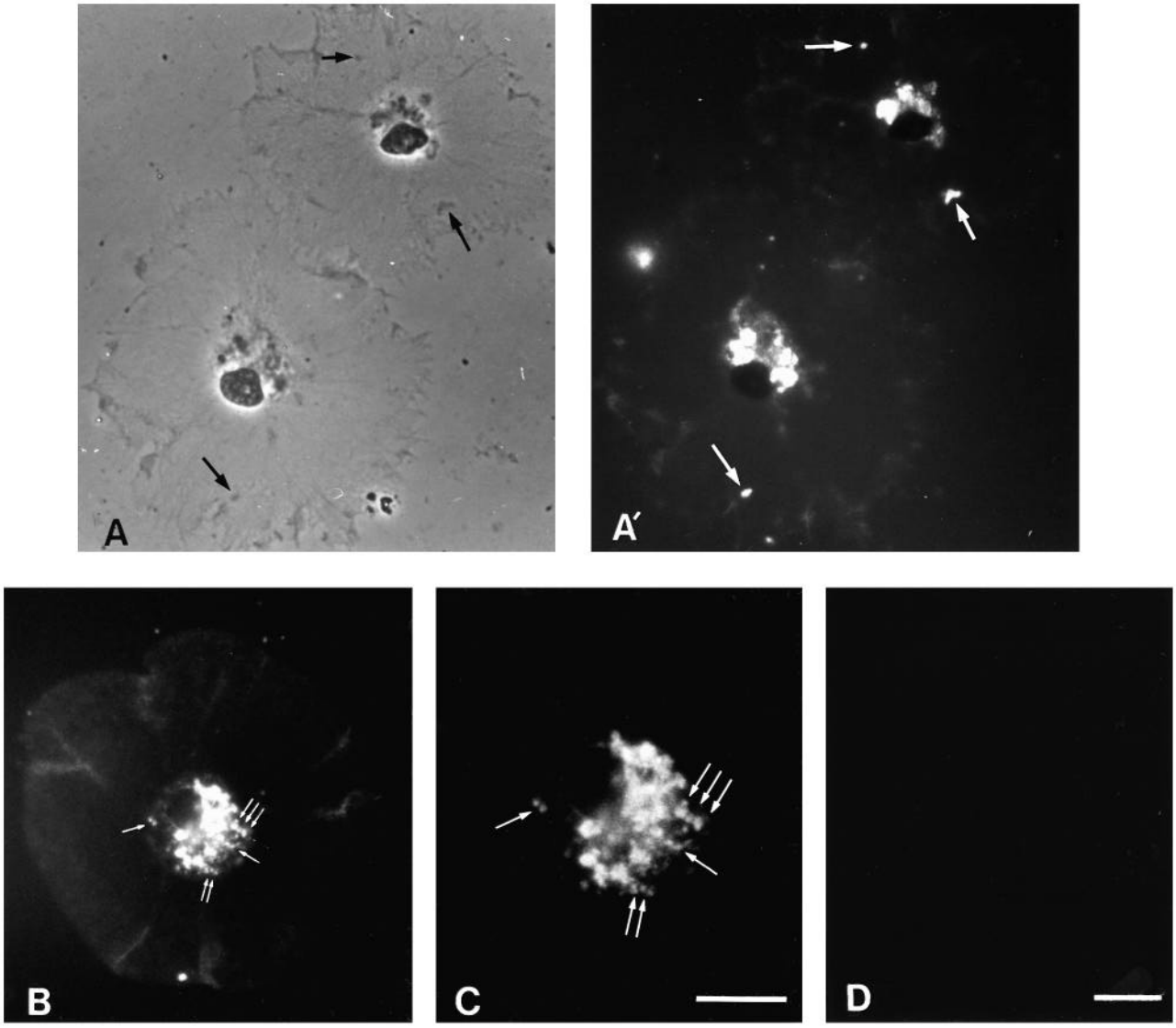

Fig. 6. Indirect immunofluorescence localization of unconventional myosin in untransformed coelomocytes. (A) Phase-contrast micrograph of coelomocytes spread down onto the coverslip, making it possible to view the perinuclear region and the large sheet-like lamellae. The majority of particles/vesicles were accumulated in the perinuclear endoplasm with an occasional particle/vesicle in peripheral lamellae. (A′) Indirect immunofluorescence micrograph of cells in A stained with the anti-brush border unconventional myosin-I antibody, revealing patches of fluorescence corresponding to phase-dense and phase-lucent particles/vesicles in the perinuclear region. The anti-brush border unconventional myosin-I antibody also stained phase-dense particles/vesicles located in the peripheral lamellae (arrows). (B) Spread coelomocyte stained with the anti-brush border unconventional myosin-I antibody identifying numerous perinuclear particles/vesicles, and a slight diffuse band of fluorescence at the lamellar edge. (C) Higher magnification of the perinuclear region of the cell in B showing the staining of individual particles/vesicles and clusters of particles/vesicles (arrows). (D) Fluorescence staining of coelomocytes with secondary antibody only. Bars, 10 μm.

Coelomocyte particle/vesicle translocation

In an effort to understand the complex mechanisms of intracellular cargo motility and myosin motor activity, we turned to the echinoderm coelomocyte because its actin and microtubule cytoskeletons have been well characterized, and the cells have been reported to undergo particle/vesicle transport. This motility model relies on the observation that petalloid coelomocytes will adhere to glass coverslips leading to a highly spread lamellar form, and when challenged with hypotonic buffer will not readily generate filopodia but instead exhibit activated particle/vesicle motility.

In hypotonically treated cells with radially arranged microtubule and microfilament networks, we observed a very broad distribution of particle/vesicle velocities ranging from 0.02 to 0.12 $\mu m\ s^{-1}$. The observed distribution appeared multi-modal and curve-fitting regression analysis demonstrated that the data were best fit to three separate Gausian velocity populations. This observation suggests the presence of discrete types of cargo motility that may be driven along actin filament or microtubule tracks. To determine if any of the observed particle/vesicle motility was dependent upon myosin-type motors, coelomocytes were treated with nocodazole to destroy

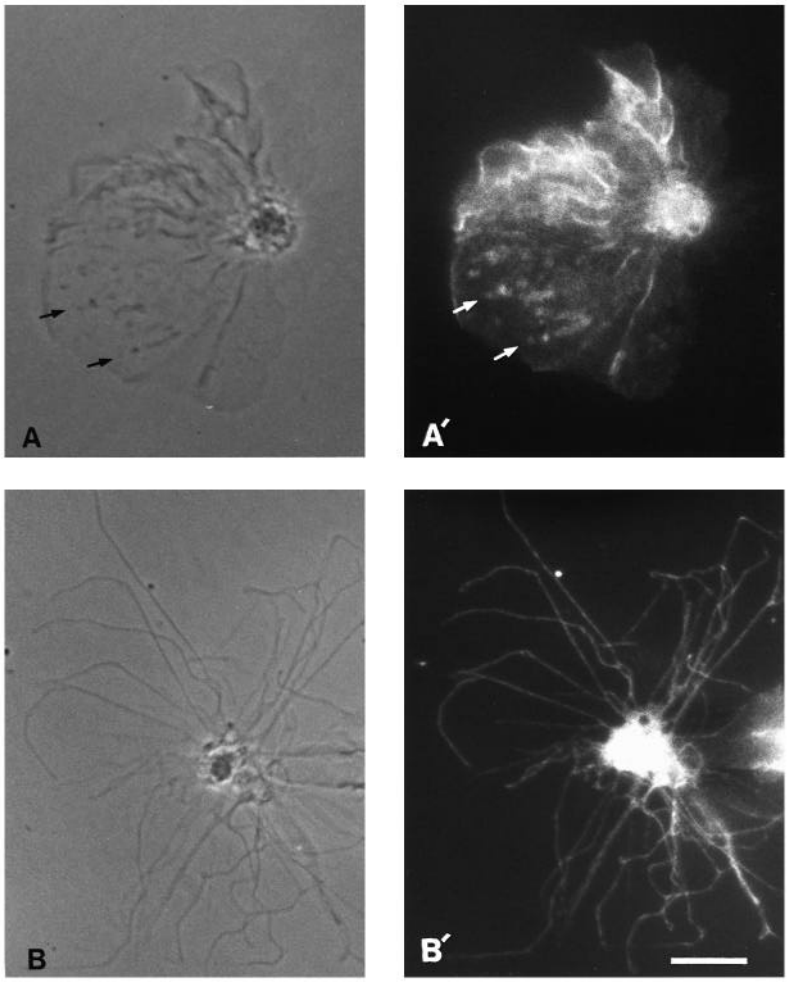

Fig. 7. Unconventional myosin localization in partially and fully transformed coelomocytes. (A) Phase-contrast micrograph of a cell in the process of transforming. (A′) Corresponding fluorescence micrograph of the partially transformed cell in A stained by indirect immunofluorescence using affinity-purified, anti-brush border unconventional myosin-I antibodies. Notice the uniform fluorescence within the perinuclear region and the distinct presence of particles/vesicles within the lamellae. In some cases, particles/vesicles appear in a linear array (arrows). (B) Phase-contrast image of a transformed coelomocytes exhibiting many surface filopodia. (B′) Companion fluorescence micrograph of the cell in B showing anti-brush border unconventional myosin-I antibody staining of the elongate filopodia. Bar, 10 μm.

radial microtubule tracks and thus eliminate motile particles/vesicles driven by microtubule-dependent motors, for example, coelomocyte kinesin (Wright et al., 1991; Henson et al., 1992). Nocodazole-treated coelomocytes continued to exhibit radial particle/vesicle motility; however, the velocity profile was much tighter than in control preparations, resulting in an average velocity of 0.028±0.006 μm s^{-1}. Statistical analysis of this velocity distribution demonstrated excellent correlation with a single Gausian distribution and thus suggests the possible presence of a single discrete class of moving particles/vesicles. Since these movements are occurring in the absence of intact microtubules, we conclude that the particles/vesicles were driven along existing actin filament tracks by a myosin-type motor. A comparison of the rhodamine-phalloidin-stained cells in Figs 1F and 2F potentially gives the impression of increased numbers of radial actin bundles in nocodazole-treated coelomocytes. From our observations, we have not been able to draw a conclusion concerning the possible reorganization or formation of radial actin filaments and bundles in response to the loss of microtubules. If such a structural change does indeed occur it may illustrate the cell's plasticity in handling an assault on its cytoskeletal transport pathways (see Lillie and Brown, 1992).

At first glance, the observed rate of actin-myosin-dependent particle/vesicle motility appeared relatively slow; however, the data were not inconsistent with the broad range of rates observed for particle/vesicle translocation by myosin motors. For example, vesicles isolated from *Acanthamoeba* moved at an average speed of 0.24 μm s^{-1} (Adams and Pollard, 1986) while velocities of 0.033 μm s^{-1} were reported for chicken brush border myosin-I membrane discs moving along *Nitella* actin cables (Mooseker et al., 1989). Faster rates were observed in extruded squid axoplasm where vesicles moved along actin filaments at velocities ranging from 0.7 to 1 μm s^{-1} (Kuznetsov et al., 1992) and by far the fastest rates observed in any system are those reported from the aquatic alga *Chara*, where vesicles move at speeds up to 62 μm s^{-1} (Kachar, 1985). The broad range of motility rates measured for myosin is assuredly a function of their biochemical regulation via calcium, calmodulin or phosphorylation, and the type of motility assay employed (Collins and Borysenko, 1984; Spudich, 1989; Brzeska et al., 1989; Collins et al., 1990; Krizek et al., 1987; Wolenski et al., 1993).

Coelomocytes having normal microtubule arrays exhibited overall faster rates of particle/vesicle movement with apparently two distinct velocities, attributed to microtubule-based motors. The simplest interpretation of such a distribution is the cellular presence of multiple microtubule plus-end-directed motor proteins. Recently, kinesin has been identified in coelomocytes and it was localized to endosomes and linear endoplasmic reticular tubules (Wright et al., 1990; Henson et al., 1992). Dynein-type motors have not been identified. The rates

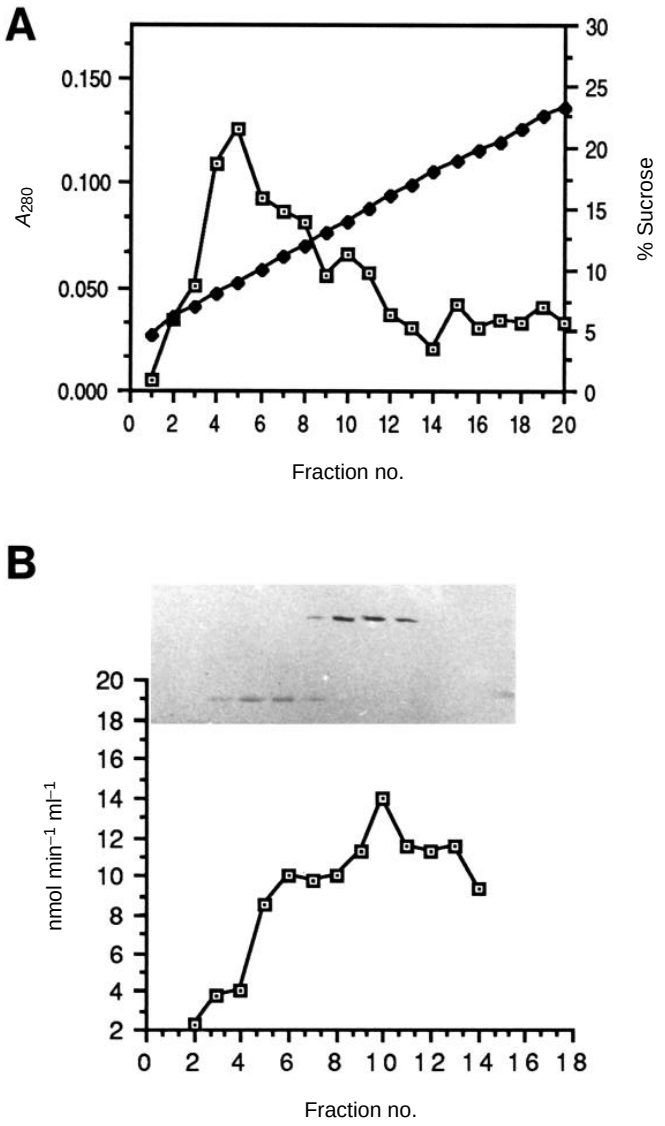

Fig. 8. Density gradient fractionation of coelomocyte lysates. (A) Graph of sucrose gradient depicting protein content (□) and % sucrose (◆) as a function of equivalent fractions removed from the top to the bottom of the gradient. (B) K^+EDTA-activated ATPase analysis of fractions across the gradient. Two peaks of activity were present, corresponding to 10% and 15% sucrose. Immunoblot of sucrose gradient fractions, using a mixture of the anti-unconventional myosin-I antibodies and anti-brush border conventional myosin-II antibodies, revealed the presence of the 110 kDa unconventional myosin (lower band) corresponding to the first peak of activity and the presence of conventional myosin-II (upper band) in the second peak of activity.

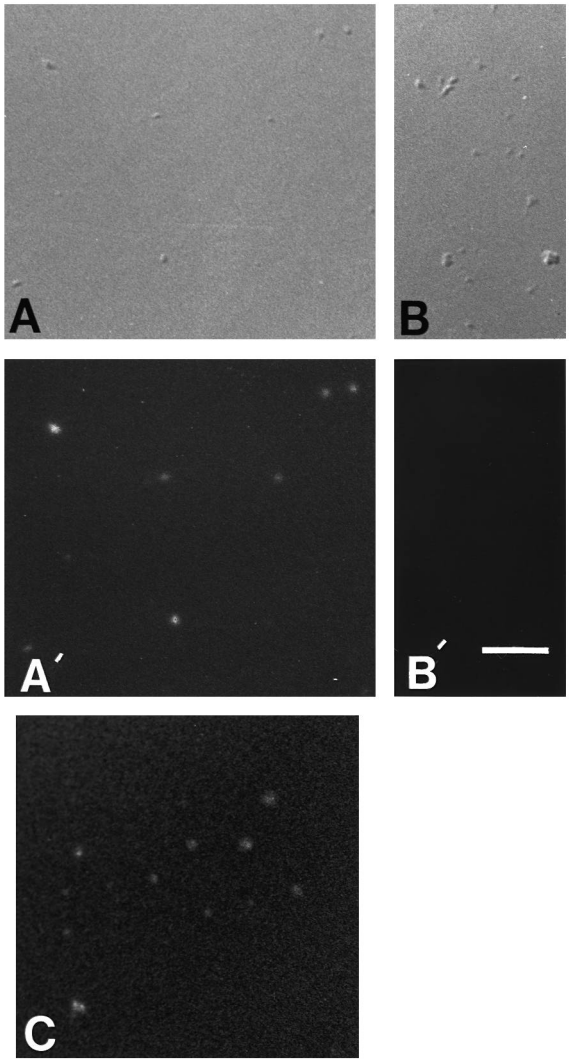

Fig. 9. Identification of unconventional 110 kDa myosin association with coelomocyte particles/vesicles. (A) DIC micrograph of particles/vesicles obtained from sucrose gradient fraction. (A′) Fluorescence micrograph of particles/vesicles in A stained by indirect immunofluorescence using affinity-purified, anti-brush border unconventional myosin-I antibodies. Notice the one to one correlation of unconventional myosin staining with particles/vesicles detected in the DIC image. (B and B′) DIC micrograph and the corresponding anti-myosin-II immunofluorescence micrograph of sucrose gradient-isolated particles/vesicles. Note the absence of any detectable anti-myosin-II antibody staining. (C) Companion preparation to A and B showing that the particles/vesicles detected by DIC were also stained with the membrane dye $DiOC_6$. Bar, 5 μm.

of microtubule-based particle/vesicle motility in coelomocytes are ~10- to 20-fold slower than the dynein and kinesin rates of microtubule-based motility observed in other systems (Brady, 1985; Brady et al., 1990; Gilbert and Sloboda, 1989). As with the myosin motor proteins, there is clearly variability among the motility rates produced by the microtubule motors and this may reflect differential regulation of motor activity by motility enhancement factors (Gill et al., 1991).

Noteworthy are the observations of particles/vesicles moving along both microtubule tracks and actin filaments in extruded squid axoplasm (Kuznetsov et al., 1992). Interestingly, particles/vesicles that moved linearly along microtubules in the axoplasmic extract could switch and begin translocating on adjacent actin filaments. At present, the motor proteins involved in track-switching motility remain unknown; however, recent reports have identified an axoplasmic barbed-end-directed actin-based motor (Bearer et al., 1993a; Langford et al., 1993) that is immunologically related to conventional myosin-II (Bearer et al., 1993b). We have no evidence for track

switching in coelomocytes during hypotonic shock-induced particle/vesicle motility; nonetheless, this still remains a possibility.

Coelomocyte unconventional myosin: a motor for driving intracellular particle/vesicle motility

As one of our initial steps toward characterizing the mechanistic basis of coelomocyte particle/vesicle motility, we examined the possibility that an unconventional myosin may be responsible for the activated motility of intracellular particles/vesicles, since immunofluorescence localization using anti-conventional myosin-II antibodies did not detect any myosin-II association with intracellular particles. In an effort to identify unconventional myosin motor proteins, coelomocyte extracts were fractionated by column chromatography and preparations enriched for a 110 kDa polypeptide were identified as possessing ATPase activity characteristic of myosin motor proteins. The actin-activated ATPase activity of the 110 kDa fractions was salt-dependent, with greater actin activation at lower ionic strength, a finding similar to the reported ionic strength dependence of brush border unconventional myosin-I activity (Collins et al., 1990; Conzelman and Mooseker, 1987; Krizek et al., 1987). Further, the 110 kDa polypeptide was found to be immuno-crossreactive with antibody probes documented to be specific for unconventional myosin-I but not conventional myosin-II (Carboni et al., 1988; Collins et al., 1990). In the absence of sequence data, we defer classification of coelomocyte unconventional myosin according to the Cheney et al. (1993) nomenclature.

Subfractionation of 'resting' coelomocytes by sucrose gradient centrifugation identified fractions that were enriched with coelomocyte 110 kDa unconventional myosin and also contained numerous particles/vesicles of approximately the same size as those observed in situ. Indirect immunofluorescence staining of the gradient fractions demonstrated that anti-brush border unconventional myosin-I antibodies labeled all the particles detected by video-DIC. Furthermore, the particles in these preparations were all stained with $DiOC_6$, a fluorescent membrane and vesicle stain (Terasaki et al., 1984; Wilson, 1985), suggesting that coelomocyte unconventional 110 kDa myosin was associated with an intracellular membrane compartment, possibly motile vesicles. In support of this hypothesis is the recent study by Henson et al. (1992), who characterized the particles/vesicles observed by light microscopy and their potential association with the microtubule motor protein kinesin. Their findings suggest that kinesin is the potential motor for endosomes and endoplasmic reticulum in coelomocytes, therefore the activity of other motor protein families must be involved in the motility of mitochondria, lysosomes, Golgi vesicles, and acidic vesicles located in lamellar and perinuclear regions. In preliminary studies of nocodazole-treated cells, outward moving particles/vesicles sequestered the mitochondrial fluorescent dye rhodamine-123 while acridine orange-labeled phase-lucent compartments remained perinuclear (Sgourdas and Bonder, unpublished observations). Future analysis of the particle/vesicle compartments that are co-localized with coelomocyte unconventional myosin should define the cargo transported via unconventional myosin motor activity and provide insight into the role of unconventional myosin during transformation.

Involvement of coelomocyte unconventional myosin in the dynamic membrane-cytoskeletal restructuring during filopod formation

The mechanism of coelomocyte transformation and the contractile elements involved in this process have been extensively studied (Otto et al., 1979; Edds and Venuti-Henderson, 1983). Regulation of transformation has been correlated to the elevation of intracellular Ca^{2+} and may involve calmodulin, which has been localized to the perinuclear region (Henson and Schatten, 1983; Hyatt et al., 1984; Venuti and Edds, 1986). The mechanism of filopodial extension proposed by Edds (1977, 1980) is a two-step process involving the bundling of actin networks and a concomitant retraction of the membrane around the elongating actin bundle whereby the filopodia can be extended up to four times their original length (Edds, 1977). As the actin filament bundles elongate during transformation, the possibility arises that additional membrane may be necessary to enclose the elongating bundles of actin filaments and that the actin bundles need to become attached to the plasma membrane. Degranulation during transformation may provide the source of plasma membrane needed to sheathe the elongating actin bundle. At present, we do not observe massive degranulation of lamellar particles/vesicles following hypotonic shock; however, we have observed what appears to be exocytosis in the perinuclear region. Since unconventional 110 kDa myosin is associated with numerous perinuclear particles/vesicles, exocytosis during the transformation process might provide plasma membrane-associated unconventional myosin for the formation and maintenance of filopodia.

The potential for unconventional myosin participation in pseudopod/filopod formation relies upon observations that these motor proteins possess both membrane- and cytoskeleton-binding capacities (reviewed by Cheney and Mooseker, 1992). For example, in polarized intestinal epithelial cells, brush border unconventional myosin-I is located on apically positioned vesicles (Drenckhahn and Dermietzel, 1988; Achler et al., 1989) and recently Fath and Burgess (1993) demonstrated the association of brush border unconventional myosin-I with Golgi-derived vesicles. It has been suggested that in epithelial cells, vesicles are translocated to the apical end of the cell via a microtubule-motor system and, subsequently, as the vesicles reach the terminal web, myosin-I then directs and translocates vesicles apically along microvillar rootlets toward the plasma membrane (Collins and Borysenko, 1984; Drenckhahn and Dermietzel, 1988; Fath et al., 1990; Fath and Burgess, 1993). Once delivered to the apical surface the myosin-I could function in zippering and tethering the apical membrane of the microvilli to the actin filament microvillar core bundles (Fath et al., 1990; Fath and Burgess, 1993; Mooseker, 1985). By analogy, during the transformation process 110 kDa unconventional myosin may translocate secretory vesicles as well as play a critical role in zippering the newly added membrane onto extending actin filament bundles within the filopodia. Another interesting possibility is that membrane-associated unconventional myosin could actually provide the motive force necessary for filopodial extension (see Sheetz et al., 1992, for extensive discussion).

Thus, the coelomocyte model possesses both microtubule- and actin microfilament-dependent motility pathways that can be experimentally distinguished and analyzed. Finally, the

stimulus/response coupling to motility may enable experimental identification of the mechanisms regulating particle/vesicle motility by unconventional myosin motor proteins.

We thank Drs Tom Pollard, Tom Keller, Kathy Collins, Paul Matsudaira and Jim Sellers for generously providing myosin antibodies. We thank the members of the Bonder Lab for critical discussions, and Dr Jim Tepper for assistance with the statistical analysis. Special thanks to the reviewers of this manuscript whose thoughtful comments were appreciated. This work was submitted in partial fulfillment of the PhD degree requirements at Rutgers University (L.D.). This study was supported by a Predoctoral Fellowship Award from the American Heart Association - NJ Affiliate (L.D.) and NIH HD 24649 (E.B.). Preliminary reports of these results were presented at the 1991 and 1992 annual meetings of the American Society for Cell Biology. Preliminary reports of these results were presented at the 1991 and 1992 annual meetings of the American Society for Cell Biology (D'Andrea and Bonder, 1991; D'Andrea et al., 1992).

REFERENCES

Achler, C., Filmer D., Merte C. and Drenckhahn, D. (1989). Role of microtubules in polarized delivery of apical membrane proteins to the brush border of the intestinal epithelium. *J. Cell Biol.* **109**, 179-189.

Adams, R. J. and Pollard, T. D. (1986). Propulsion of organelles isolated from *Acanthamoeba* along actin filaments by myosin-I. *Nature* **322**, 754-756.

Allen, R. D., Zacharski, L. R., Widirski, S. T., Rosenstein, R., Zaitlin, L. M. and Burgess, D. R. (1979). Transformation and motility of human platelets. *J. Cell Biol.* **83**, 126-142.

Baines, I. C., Brzeska, H. and Korn, E. D. (1992). Differential localization of *Acanthamoeba* myosin-I isoforms. *J. Cell Biol.* **119**, 1193-1203.

Bearer, E. L., DeGiorgis, J. A., Kao, A. W., Bodner, R. A. and Reese, T. S. (1993a). Evidence for an actin motor in isolated squid axoplasm. *Mol. Biol. Cell* **227a**.

Bearer, E. L., DeGiorgis, J. A., Kao, A. W., Bodner, R. A. and Reese, T. S. (1993b). Evidence for myosin motors on organelles in squid axoplasm. *Proc. Nat. Acad. Sci. USA* **90**, 11252-11256.

Bement, W. M. and Mooseker, M. S. (1993). Molecular motors: keeping out the rain. *Nature* **365**, 785-786.

Bradford, M. M. (1976). A rapid and sensitive method for the quantitation of microgram quantities of protein using the principle of protein-dye binding. *Anal. Biochem.* **72**, 248-254.

Brady, S. T. (1985). A novel brain ATPase with properties expected for the fast axonal transport motor. *Nature* **317**, 73-75.

Brady, S. T., Pfister, K. K. and Bloom, G. S. (1990). A monoclonal antibody against kinesin inhibits both anterograde and retrograde fast axonal transport in squid axoplasm. *Proc. Nat. Acad. Sci. USA* **87**, 1061-1065.

Bray, D. and Vasiliev, J. M. (1989). Networks from mutants. *Nature* **338**, 203-204.

Brzeska, H., Lynch, T. J., Martin, B. and Korn, E. D. (1989). The localization and sequence of the phosphorylation sites of *Acanthamoeba* myosins-I. *J. Biol. Chem.* **264**, 19340-19348.

Canicatti, C., Pagliara, P. and Stabili, L. (1992). Sea urchin coelomic fluid agglutinin mediates coelomic adhesion. *Eur. J. Cell Biol.* **58**, 291-295.

Carboni, J. M., Conzelman, K. A., Adams, R. A., Kaiser, D. A., Pollard, T. D. and Mooseker, M. S. (1988). Structural and immunological characterization of the myosin-like 110kD subunit of the intestinal microvillar 110kD-calmodulin complex: evidence for discrete myosin head and calmodulin binding domains. *J. Cell Biol.* **107**, 1749-1757.

Cheney, R. E. and Mooseker, M. S. (1992). Unconventional myosins. *Curr. Opin. Cell Biol.* **4**, 27-35.

Cheney, R. E., Riley, M. A. and Mooseker, M. S. (1993). A phylogenic analysis of the the myosin superfamily. *Cell Motil. Cytoskel.* **24**, 215-223.

Coffaro, K. A. and Hinegardner, R. (1977). Immune response in the sea urchin *Lytechinus pictus. Science* **197**, 1389-1390.

Collins, J. H. and Borysenko, C. W. (1984). The 110,000 dalton actin and calmodulin binding protein from intestinal brush border is a myosin-like ATPase. *J. Biol. Chem.* **259**, 14128.

Collins, K., Sellers, J. R. and Matsudaira, P. (1990). Calmodulin dissociation regulates brush border myosin-I (110-kD-calmodulin) mechanochemical activity *in vitro. J. Cell Biol.* **110**, 1137-1147.

Conzelman, K. A. and Mooseker, M. S. (1987). The 110 kDa protein-calmodulin complex of the intestinal microvillus is an actin-activated MgATPase. *J. Cell Biol.* **105**, 313-324.

D'Andrea, L. and Bonder, E. M. (1991). Identification of myosin-I-like proteins in sea urchin coelomocytes and eggs. *J. Cell Biol.* **115**, 331a.

D'Andrea, L., Danon, M. and Bonder, E. M. (1992). Biochemical analysis of sea urchin coelomocyte myosin-I and -II. *Mol. Biol. Cell* **3**, 46a.

D'Andrea, L. (1993). Biochemical, morphological, and structural examination of actin-based motility in echinoderm sperm, eggs, and immune coelomocytes: analysis of dynamic actin-membrane reorganizations involving spectrin, myosin-I, and myosin-II. PhD thesis, Rutgers University.

Doberstein, S. K. and Pollard, T. D. (1992). Localization and specificity of the phospholipid and actin binding sites on the tail of *Acanthamoeba* myosin-IC. *J. Cell Biol.* **117**, 1241-1249.

Doberstein, S. K., Baines, I. C., Wiegand, G., Korn, E. D. and Pollard, T. P. (1993). Inhibition of contractile vacuole function in vivo by antibodies against myosin-I. *Nature* **365**, 841-843.

Drenckhahn, D. and Dermietzel, R. (1988). Organization of the actin filament cytoskeleton in the intestinal brush border: a quantitative and qualitative immunoelectron microscopic study. *J. Cell Biol.* **107**, 1037-1048.

Dubreuil, R., Byers, T. J., Branton, D., Goldstein, L. S. B. and Kiehart, D. P. (1987). *Drosophila* spectrin. I. Characterization of the purified protein. *J. Cell Biol.* **105**, 2095-2102.

Edds, K. T. (1977). Dynamic aspects of filopodial formation by reorganization of microfilaments. *J. Cell Biol.* **73**, 479-491.

Edds, K. T. (1980). The formation of filopodia during transformation of sea urchin coelomocytes. *Cell Motil.* **1**, 131-140.

Edds, K. T. and Venuti-Henderson, J. (1983). Coelomocyte spectrin. *Cell Motil.* **3**, 683-691.

Edds, K. T. (1984). Differential distribution and function of microtubles and microfilaments in sea urchin coelomocytes. *Cell Motil.* **4**, 269-281.

Edds, K. T. (1993). Effects of cytochalasin and colcemid on cortical flow in coelomocytes. *Cell Motil. Cytoskel.* **26**, 262-273.

Endean, R. (1966). In *Physiology of Echinodermata* (ed. R. A. Boolootian), pp. 301-328. New York: J. Wiley & Sons.

Endow, S. A. and Titus, M. A. (1992). Genetic approaches to molecular motors. *Annu. Rev. Cell Biol.* **8**, 29-66.

Fath, K. R., Obenauf, S. D. and Burgess, D. R. (1990). Cytoskeletal protein and mRNA accumulation during brush border formation in adult chicken enterocytes. *Development* **109**, 449-459.

Fath, K. R. and Burgess, D. R. (1993). Golgi-derived vesicles from developing epithelial cells bind actin filaments and possess myosin-I as a cytoplasmically-oriented peripheral membrane protein. *J. Cell Biol.* **120**, 117-127.

Forscher, P., Lin, C. H. and Thompson, C. (1992). Novel form of growth cone motility involving site-directed actin filament assembly. *Nature* **357**, 515-518.

Gilbert, S. P. and Sloboda, R. D. (1989). A squid dynein isoform promotes axoplasmic vesicle translocation. *J. Cell Biol.* **109**, 2379-2394.

Gill, S. R., Schroer, T. A., Szilak, I., Steuer, E., Sheetz, M. and Cleveland, D. W. (1991). Dynactin, a conserved, ubiquitously expressed component of an activator of vesicle motility mediated by cytoplasmic dynein. *J. Cell Biol.* **115**, 1639-1650.

Hayden, S. M., Wolenski, J. S. and Mooseker, M. S. (1990). Binding of brush border myosin-I to phospholipid vesicles. *J. Cell Biol.* **111**, 443-451.

Henson, J. H. and Schatten, G. (1983). Ca^{2+} regulation of the actin mediated cytoskeletal transformation of sea urchin coelomocytes. *Cell Motil.* **3**, 525-534.

Henson, J. H., Nesbitt, D., Wright, B. D. and Scholey, J. M. (1992). Immunolocalization of kinesin in sea urchin coelomocytes. *J. Cell Sci.* **103**, 309-320.

Hyatt, H. A., Shure, M. S. and Begg, D. A. (1984). Induction of shape transformation in sea urchin coelomocytes by the calcium ionophore A23187. *Cell Motil.* **4**, 57-71.

Johnson, P. (1969). The coelomic elements of sea urchins (*Strongylocentrotus*). I. The normal coelomocytes: their morphology and dynamics in hanging drops. *J. Invert. Path.* **13**, 25-41.

Jung, G. and Hammer, J. A. III (1990). Generation and characterization of *Dictyostelium* cells deficient in a myosin-I heavy chain isoform. *J. Cell Biol.* **110**, 1955-1964.

Kachar, B. (1985). Direct visualization of organelle movement along actin filaments dissociated from Characean algae. *Science* **227**, 1355-1357.
Kellerman, K. A. and Miller, K. G. (1992). An unconventional myosin heavy chain gene from *Drosophila melanogaster*. *J. Cell Biol.* **119**, 823-834.
Kiehart, D. P., Kaiser, D. A. and Pollard, T. D. (1984). Monoclonal antibodies demonstrate limited structural homology between myosin isozymes from Acanthamoeba. *J. Cell Biol.* **99**, 1002-1014.
Korn, E. D. and Hammer, J. A. III (1990). Myosin-I. *Curr. Opin. Cell Biol.* **2**, 57-61.
Krizek, J., Coluccio, L. M. and Bretscher, A. (1987). ATPase activity of the microvillar 110 kDa polypeptide-calmodulin complex is activated in Mg^{2+} and inhibited in K^{+}EDTA by F-actin. *FEBS Lett.* **225**, 269-272.
Kuznetsov, S., Langford, G. M. and Weiss., D. G. (1992). Actin-dependent organelle movement in squid axoplasm. *Nature* **356**, 722-725.
Laemmli, U. K. (1970). Cleavage of structural proteins during the assembly of the head of the bacteriophage T4. *Nature* **314**, 472-474.
Langford, G. M., Kuznetsov, S. A., Johnson, D. A., Cohen, D. L. and Weiss, D. G. (1993). Axoplasmic organelles move toward the barbed end of actin filaments. *Mol. Biol. Cell* **275a**.
Lillie, S. H. and Brown., S. S. (1992). Suppression of a myosin defect by a kinesin-related gene. *Nature* **356**, 358-361.
Mabuchi, I. (1976). Myosin from starfish egg: properties and interaction with actin. *J. Mol. Biol.* **100**, 569-582.
Matsudaira, P. T. and Burgess, D. R. (1978). SDS micro-slab linear gradient polyacrylamide gel electrophoresis. *Anal. Biochem.* **87**, 386-396.
Mooseker, M. S. (1985). Organization, chemistry and assembly of the cytoskeletal apparatus of the intestinal brush border. *Annu. Rev. Cell Biol.* **1**, 209-241.
Mooseker, M. S., Conzelman, K. A., Coleman, T. R., Heuser, J. E. and Sheetz, M. P. (1989). Characterization of intestinal microvillar membrane disks: detergent resistant membrane sheets enriched in associated brush border myosin-I (110K-calmodulin). *J. Cell Biol.* **109**, 1153-1161.
Noegel, A. A. and Schleicher, M. (1991). Phenotypes of cells with cytoskeletal mutations. *Curr. Opin. Cell Biol.* **3**, 18-26.
Otto, J. J., Kane, R. and Bryan, J. (1979). Formation of filopodia in coelomocytes: localization of fascin, a 58,000 dalton actin crosslinking protein. *Cell* **17**, 285-293.
Platt, J. L. and Michael, A. F. (1983). Retardation of fading and enhancement of intensity of immunofluorescence by p-phenylenediamine. *J. Histochem. Cytochem.* **31**, 840-842.
Pollard, T. D. and Korn, E. D. (1973). *Acanthamoeba* myosin. Isolation from *Acanthamoeba* of an enzyme similar to muscle myosin. *J. Biol. Chem.* **248**, 4682-4690.
Pollard, T. D., Doberstein, S. K. and Zot, H. G. (1991). Myosin-I. *Annu. Rev. Physiol.* **53**, 653-681.
Ryoyama, K. (1974). Studies on the biological properties of coelomic fluid of sea urchin. II. Naturally occurring hemagglutinin in sea urchin. *Biol. Bull. Mar. Biol. Lab., Woods Hole* **146**, 404-414.
Sheetz, M. P., Wayne, D. B. and Pearlman, A. L. (1992). Extension of filopodia by motor-dependent actin assembly. *Cell Motil. Cytoskel.* **22**, 160-162.
Spudich, J. A. (1989). In pursuit of myosin function. *Cell Regul.* **1**, 1-11
Terasaki, M., Song, J., Wong, J. R., Weiss, M. J. and Chen, L. B. (1984). Localization of endoplasmic reticulum in living and gluteraldehyde fixed cells with fluorescent dyes. *Cell* **38**, 101-108.
Titus, M. A. (1993). Myosins. *Curr. Opin. Cell Biol.* **5**, 77-81.
Titus, M. A., Wessels, D., Spudich, J. A. and Soll, D. (1993). The unconventional myosin encoded by the myoA gene plays a role in *Dictyostelium* motility. *Mol. Biol. Cell.* **4**, 233-246.
Towbin, H., Staehelin, T. and Gordon, J. (1979). Electrophoretic transfer of protein from polyacrylamide gels to nitrocellulose sheets: Procedure and some application. *Proc. Nat. Acad. Sci. USA* **76**, 4350-4354.
Venuti, J. M. and Edds, K. T. (1986). Calmodulin and calmodulin binding proteins in the morphological transformation of sea urchin coelomocytes. *Cell Motil. Cytoskel.* **6**, 604-619.
Wagner, M. C., Barylko, B. and Albanesi, J. P. (1992). Tissue distribution and subcellular localization of mammalian myosin-I. *J. Cell Biol.* **119**, 163-170.
Warrick, H. M. and Spudich, J. A. (1987). Myosin structure and function in cell motility. *Annu. Rev. Cell Biol.* **3**, 379-421.
Wessels, D., Murray, J., Jung, G., Hammer III, J. A. and Soll, D. A. (1991). Myosin-IB null mutants of *Dictyostelium* exhibit abnormalities in motility. *Cell Motil. Cytoskel.* **20**, 301-315.
Wilson, H. A. (1985). Voltage sensitive cyanine dye fluorescence signal in lymphocytes: plasma membrane and mitochondral components. *J. Cell. Physiol.* 125, 61-69.
Witke, W., Schleicher, M. and Noegel, A. A. (1992). Redundancy in the microfilament system: abnormal development of *Dictyostelium* cells lacking two F-actin cross-linking proteins. *Cell* **68**, 53-62.
Wolenski, J. S., Hayden, S. M., Forscher, P. and Mooseker, M. S. (1993). Calcium-calmodulin and regulation of brush border myosin-I MgATPase and mechanochemistry. *J. Cell Biol.* **122**, 601-612.
Wright, B. D., Henson, J. H., Wedaman, K. P., Willy, P. J., Morand, J. N. and Scholey, J. M. (1991). Subcellular localization and sequence of sea urchin kinesin heavy chain: evidence for its association with membranes in the mitotic apparatus and interphase cytoplasm. *J. Cell Biol.* **113**, 817-834.
Yonemura, S. and Pollard, T. D. (1992). The localization of myosin-I and myosin-II in *Acanthamoeba* by fluorescence microscopy. *J. Cell Sci.* **102**, 629-642.
Yui, M. A. and Bayne, C. (1983). Echinoderm immunology: bacterial clearance by sea urchin *S. purpuratus*. *Biol. Bull. Mar. Biol. Lab., Woods Hole* **165**, 473-486.
Zot, H. G., Doberstein, S. K. and Pollard, T. D. (1992). Myosin-I moves actin filaments on a phospholipid substrate: Implications for membrane targeting. *J. Cell Biol.* **116**, 367-376.

(Received 17 February 1994 - Accepted 2 May 1994)